

Signature of Electron-Phonon Correlation in the Band Structure of $\text{Sr}_4\text{Ru}_3\text{O}_{10}$

P. Ngabonziza, E. Carleschi and B.P. Doyle

Department of Physics, University of Johannesburg, P.O. Box 524 Auckland Park 2006, Johannesburg, South Africa

E-mail: ecarleschi@uj.ac.za

Abstract. We report the first angle resolved photoemission spectroscopy measurements on the three-layered strontium ruthenate $\text{Sr}_4\text{Ru}_3\text{O}_{10}$. These data reveal the presence of kinks in the near-Fermi-level band dispersion, with energies ranging from 30 meV to 69 meV. The kink energies have a good correspondence with the energy of the phononic modes previously reported by Raman spectroscopy measurements and lattice dynamic calculations. We interpret this as the fingerprint of strong electron-phonon coupling present in this system.

1. Introduction

In correlated electron systems, electronic excitations are characterized by an energy E and a momentum $\hbar k$ which are related through the dispersion relation $E(k)$. The interactions of electrons with other excitations, such as phonons or spin excitations, may produce anomalies in the dispersion relation that lead to sudden changes, referred to as *kinks*, in the slope of the energy-momentum dispersion close to the Fermi-level. The kink energies are often related to the relevant energy scales present in the investigated system, such as the coupling of electrons with other excitations. In particular, when relevant phonon modes are present in the system, investigation of kink energies can give rich information about the electron-phonon coupling present in the compound.

In numerous works on strongly correlated electron systems, a detailed analysis of the quasiparticle band dispersion has been performed and the existence of kinks has been revealed at energies within 100 meV from the Fermi level [1, 2]. For high- T_c cuprate superconductors in particular, kinks have been intensively investigated in order to clarify and understand the coupling mechanism that leads to superconductivity in these compounds [3]. In some cases, multiple coexisting energy scales were reported in the kink behaviour of these compounds [4]. For example, in Bi-based high- T_c cuprate superconductors, the kink in the normal state was reported to be at an energy of approximately 40 meV, while this energy increases to approximately 70 meV in the superconducting state [5]. Nonetheless, a general agreement on the origin of the behaviour of kinks in band dispersions of the high- T_c cuprates has not yet been reached and the interpretation of kinks has been controversial in these systems. In some cases the presence of kinks was attributed to an electron-phonon coupling [6, 7], while in others their presence was linked to spin-fluctuation-based ordering mechanisms [8, 9]. More recently, a novel, purely electronic mechanism leading to kinks has been reported, which does not require any coupling to phonons or other excitations but only a three-peak structure in the spectral function $\mathcal{A}(k, \omega)$

[10]. This proposed mechanism applies to correlated systems such as transition metal oxides, and can account for kinks at energies as high as a few hundred meV from the Fermi level, beyond any phononic energy scale.

Kinks have also been reported in the band dispersion of other correlated systems such as colossal magnetoresistance compounds [11], f -electron systems [12] and in single (Sr_2RuO_4) [13, 14] and double ($\text{Sr}_3\text{Ru}_2\text{O}_7$) [15] layered strontium ruthenates. In particular, the kinks resolved in band dispersions of Sr_2RuO_4 and $\text{Sr}_3\text{Ru}_2\text{O}_7$ have the same energy scale as the kinks in the high- T_c superconductors.

The three-layered strontium ruthenate $\text{Sr}_4\text{Ru}_3\text{O}_{10}$ has been reported to order ferromagnetically below $T_c \sim 105$ K, while it shows anisotropic magnetic behaviour below $T_M \simeq 65$ K: its magnetic susceptibility further increases below T_M for magnetic fields applied along the c -axis, while it decreases when the magnetic fields are applied along the ab -plane with evidence of a metamagnetic transition [16, 17]. Such behaviour was suggested to originate from the rearrangement of electrons in Ru $4d$ orbitals due to the increased dimensionality and lattice distortions in this compound [18]. Iliev *et al.* [19] performed Raman spectroscopy measurements on $\text{Sr}_4\text{Ru}_3\text{O}_{10}$. They observed Raman lines of A_g and B_{1g} symmetry, assigned to particular atomic vibrations. In particular, the B_{1g} phonon mode was associated to the internal vibrations of the RuO_6 octahedra, while the A_g phonon mode was related to the in-plane rotations of the middle RuO_6 octahedra and to the out-of-plane vibrations of O, Ru and Sr atoms. The Raman lines of B_{1g} symmetry were found to show a hardening with the ferromagnetic ordering at 105 K. Furthermore, Gupta *et al.* [20] performed magnetic field-dependent Raman measurements, where they observed significant changes in the B_{1g} phonon frequency while decreasing the temperature near T_c and around the second transition temperature T_M . All these behaviours were interpreted as a evidence of the presence of spin-phonon coupling in this compound.

In this work we report the first observation of kinks in the electronic band dispersion of $\text{Sr}_4\text{Ru}_3\text{O}_{10}$ by means of high-resolution angle resolved photoemission spectroscopy (ARPES). We resolved five different kink features, whose energies were found to be very close to the energies of the previously reported vibrational states detected by Raman spectroscopy measurements and lattice dynamics calculations (LDC) [19]. This is interpreted as evidence for strong electron-phonon coupling in this system.

2. Experimental

$\text{Sr}_4\text{Ru}_3\text{O}_{10}$ single crystals were grown using the flux-feeding floating zone technique with Ru self-flux. The growth conditions are reported elsewhere [21]. The quality of the crystals was checked using X-ray diffraction, resistivity and energy dispersive microscopy, and the samples were found to be pure single crystals of $\text{Sr}_4\text{Ru}_3\text{O}_{10}$. The ARPES measurements were performed at the beamline CASSIOPÉE of the synchrotron facility SOLEIL in Paris (France) using a Scienta R4000 electron energy analyser, which allowed us to measure simultaneously many energy distribution curves (EDC) in an angular range of 30° . The samples were cleaved *in situ* at a pressure of approximately 2×10^{-10} mbar and kept at a constant temperature of 5 K throughout the experiment. The spectra presented here were measured with a photon energy of 60 eV. The overall energy and angular resolutions were 21 meV (as confirmed by the broadening of the Fermi level) and 0.1° , respectively.

3. Results and Discussion

In figures 1a-e (upper panels) we show raw ARPES intensity cuts for selected positions in the first Brillouin zone (BZ) in a direction parallel to the Γ -X high symmetry line. Focusing on the spectral features indicated by red arrows, one observes that they disperse upward in energy with decreasing momentum. The photoemission intensity distribution of these bands varies, some of

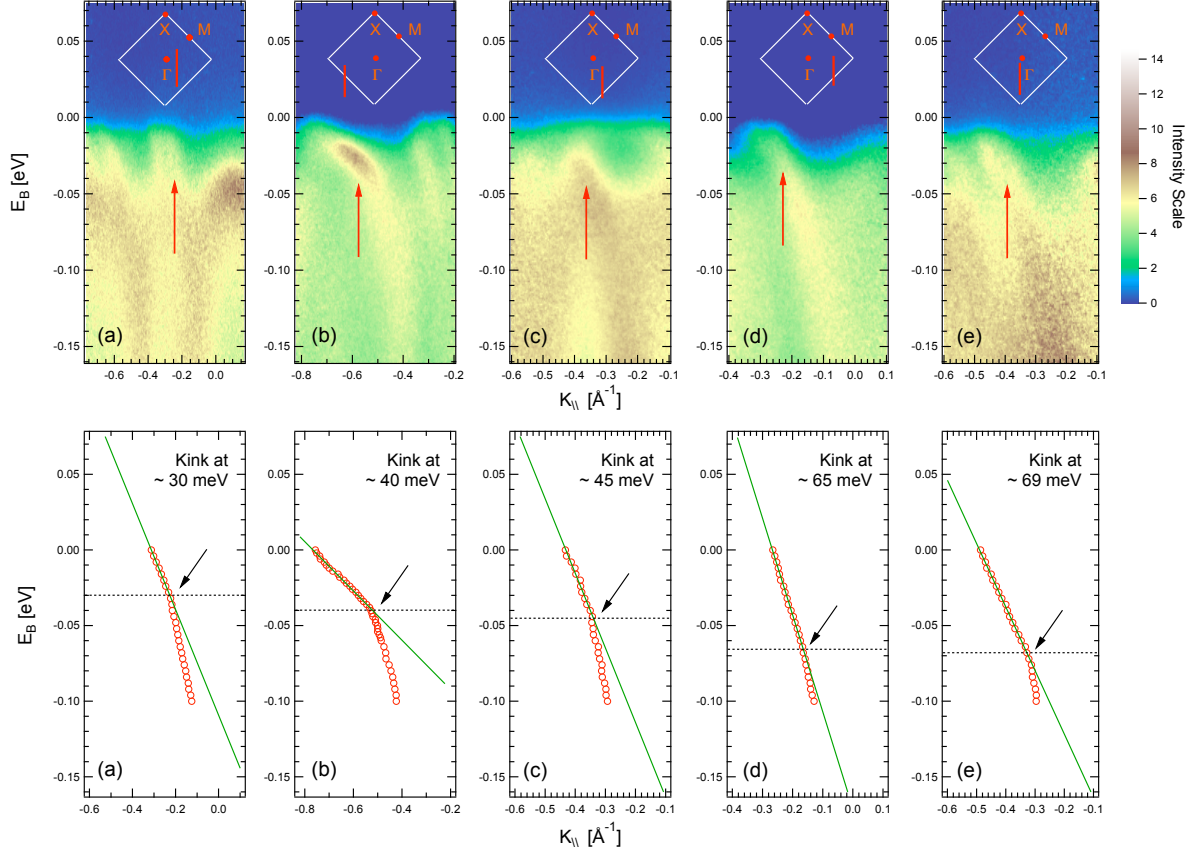


Figure 1. (Upper panels) ARPES intensity cuts measured at different positions in the first Brillouin zone. The red arrow in each cut indicates the band of interest. The rotated square at the top of each cut is a drawing of the first BZ of $\text{Sr}_4\text{Ru}_3\text{O}_{10}$. The position of the X, M, and Γ high symmetry points in the first BZ is also indicated. The red vertical line on the BZ shows the position and the direction in which the corresponding cut was acquired. (Lower panels) Experimental dispersion (red circles) extracted from the fitting of the MDC's extrapolated from cuts in the upper panels for the band of interest. Black arrows point to where kinks are observed. The green straight lines represent the fit to the low energy data.

them are more enhanced and better resolved (see for example figure 1b) as they approach the Fermi-level than others (see for example figure 1a).

In order to make a quantitative analysis of the behaviour of these spectral features as they approach the Fermi-level, we have fitted the momentum distribution curves (MDC's) extracted from the two-dimensional images with Lorentzian line shapes. Figure 2a shows the series of MDC's extracted from figure 1b top panel, while in figure 2b we show an example of such fitting, where the Lorentzian peak for the band of interest is also reported. As one can see from 2a, the line shape is rendered complicated by the presence of several features in the momentum region of interest. The positions of the MDC maxima for the particular band of interest have been followed down to a binding energy of -0.1 eV, and are plotted as a function of the binding energy in the lower panel of figure 1. This is a commonly used technique to obtain the experimental dispersion from ARPES intensity maps [22]. We observe a deviation (the so-called kink) of the dispersion from a straight line passing through the Fermi momentum k_F - represented by a dashed green line - in all the five bands. In order to obtain these kink energies, the low energy parts of

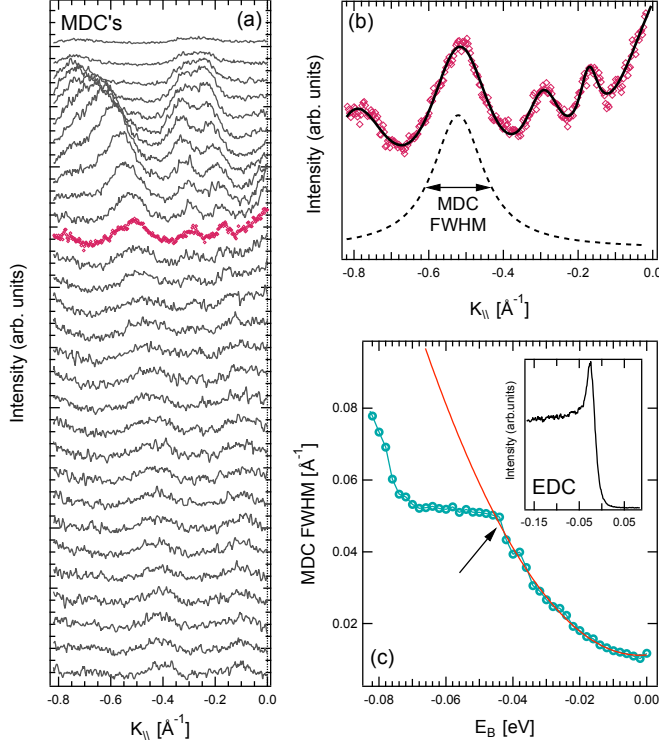


Figure 2. (a) Series of MDC spectra extracted from figure 1b by integrating over an energy range of 10 meV in 2 meV steps. The MDC spectrum in purple symbols is reported separately in (b) together with the overall fitting (solid black line) performed with Lorentzian line shapes. The Lorentzian peak for the band of interest is also reported separately (dashed black line). (c) MDC FWHM for the band of interest in figure 1b plotted versus the binding energy of the peak. The dashed red curve represents a quadratic fit to the low-energy data. The arrow marks the position of the kink. The inset shows a typical energy distribution curve (EDC) for the same peak illustrating the high resolution of these measurements.

the experimental dispersions close to the Fermi-level were fitted with straight lines (see green straight lines in figure 1), and the kink energy is taken as where the MDCs peak maxima starts to deviate significantly from the near-Fermi-level linear dispersion (indicated by black arrows). After a careful analysis of each of these experimental dispersions, we extracted the values of the kink energies of approximately 30, 40, 45, 65 and 69 meV. This energy range is comparable with what was previously reported for the low energy kinks in the high- T_c superconductors. Moreover, our results are consistent with the 40-meV kink reported for Sr_2RuO_4 and $\text{Sr}_3\text{Ru}_2\text{O}_7$ [13].

The presence of kinks is also confirmed by the plot of the MDC full width at half maximum (FWHM) versus the binding energy of the peaks. Figure 2c represents the plot for the band of interest in figure 1b. The FWHM of the MDC's is directly proportional to the imaginary part of the self energy [22], which represents the scattering rate of the quasiparticles in the system. As one can see, the scattering rate shows a discontinuity at an energy of 43 meV, which is in

ARPES Kinks [†] (meV)	30 ± 3	40 ± 2	45 ± 2	65 ± 1	69 ± 4
Raman spectroscopy * (meV)	29.15 (A_g)	38.08 (B_{1g})	47.1 (B_{1g})	-	72.95 (A_g)
Theory-LDC * (meV)	28.66 (A_g)	40.5 (B_{1g})	43.92 (B_{1g})	63.52 (A_g)	68.48 (A_g)

Table 1. Comparative table of experimental ARPES kink energies from this study ([†]) with the phonon mode obtained in the previous Raman spectroscopy study together with lattice dynamic calculations (*) from ref. [19].

very good agreement with the 40-meV kink observed for this particular feature. The low energy part of the curve can be fitted with a quadratic low energy behaviour ($\text{FWHM} \propto E^2$, solid red curve), which is thought to be a signature of the presence of quasiparticles in a Fermi liquid type in the system [22].

In order to understand the origin of the kinks in low energy band structure of $\text{Sr}_4\text{Ru}_3\text{O}_{10}$, we compare in table 1 the kink energies obtained in this ARPES study to the phonon modes observed in the previous Raman spectroscopy study and lattice dynamic calculations from ref. [19]. The symmetry of the Raman modes, either B_{1g} or A_g , is also indicated in the table. The comparison shows that the kink energies resolved in our ARPES data are approximately equal to the energy of the phononic modes, revealing a compatibility between their energy scales. In particular, the 380 cm^{-1} B_{1g} phonon mode, which was found in ref. [19] to demonstrate evidence of a structural contribution to magnetic order in $\text{Sr}_4\text{Ru}_3\text{O}_{10}$, corresponds approximately to the ARPES kink of 45 meV. We interpret these observations as being due to a strong coupling between electrons and phonons in this compound.

Acknowledgements

We are grateful to R. Fittipaldi, A. Vecchione and V. Granata for providing the single crystals for the measurements, M. Cuoco, V.B. Zabolotnyy and S. Borisenko for useful discussion, and A. Taleb-Ibrahimi and F. Bertran for technical support during the experiment. We acknowledge financial support from the South African National Research Foundation (NRF) through travel grant no. 74033.

References

- [1] M. Hengsberger *et al.* *Phys. Rev. Lett.* **83**, 592 (1999).
- [2] T. Valla *et al.* *Phys. Rev. Lett.* **83**, 2085 (1999).
- [3] E. Rotenberg *et al.* *Phys. Rev. Lett.* **84**, 2925 (2000).
- [4] W. Meevasana *et al.* *Phys. Rev. B* **75**, 174506 (2007).
- [5] T. Cuk *et al.* *Phys. Rev. Lett.* **93**, 117003 (2004).
- [6] A. Lanzara *et al.* *Nature* **412**, 510 (2001).
- [7] Z. X. Shen *et al.* *Philos. Mag. B* **82**, 1349 (2002).
- [8] H. He *et al.* *Phys. Rev. Lett.* **86**, 1610 (2001).
- [9] M. Norman *et al.* *Nature* **427**, 692, (2004).
- [10] K. Byczuk *et al.* *Nature* **3**, 168 (2007).
- [11] Z. Sun *et al.* *Phys. Rev. Lett.* **97**, 056401 (2006).
- [12] T. Durakiewicz *et al.* *Europhys. Lett.* **65**, 816, (2004).
- [13] Y. Aiura *et al.* *Phys. Rev. Lett.* **93**, 117005, (2004).
- [14] H. Iwasawa *et al.* *Phys. Rev. B* **72**, 104514, (2005).
- [15] H. Iwasawa *et al.* *Physica C* **445**, 73, (2006).
- [16] Z. Q. Mao *et al.* *Phys. Rev. Lett.* **96**, 077205 (2005).
- [17] D. Fobes *et al.* *Phys. Rev. B* **75**, 094429 (2007).
- [18] M. Malvestuto *et al.* *Phys. Rev. B* **83**, 165121 (2011).
- [19] M. N. Iliev *Physica B* **358**, 138, (2005).
- [20] R. Gupta *et al.* *Phys. Rev. Lett.* **96**, 067004, (2006).
- [21] R. Fittipaldi *Cryst. Growth and Design* **7**, 2495, (2007).
- [22] A. A. Kordyuk *et al.* *Phys. Rev. Lett.* **97**, 017002 (2006).